ISSN 0208-7774 TRIBOLOGIA 5/2019 p. 125–133
DOI: 10.5604/01.3001.0013.6569

Tomasz ŻOCHOWSKI*, Artur OLSZEWSKI**

THEORETICAL AND EXPERIMENTAL INVESTIGATION OF THIN-WALLED BEARING SHELL'S DESIGN PARAMETERS AND ASSEMBLY CONDITIONS ON THE HOLDING TORQUE INSIDE A HOUSING BORE OF A CONNECTING ROD

BADANIA TEORETYCZNE I DOŚWIADCZALNE WPŁYWU PARAMETRÓW KONSTRUKCYJNYCH ORAZ WARUNKÓW MONTAŻU PANEWKI CIENKOŚCIENNEJ NA WARTOŚĆ MOMENTU UTWIERDZENIA W GNIEŹDZIE

Key words: bearing shell, crush, test stand, experimental test, FEM simulation.

Abstract The aim of the work was the experimental and theoretical evaluation of the influence of the most important parameters determining the holding torque of a thin-walled bearing shell inside a housing bore of a connecting rod. The main investigated parameters were defined by authors experience in this field. In the first stage of research, a special test stand was designed in order to allow measuring the real values of the friction torque for different variants of bearing shell geometries and assembly conditions, additionally analysing the influence of the locking lip. Subsequently, theoretical computer-assisted FEM simulations were performed.

Słowa kluczowe: panewka cienkościenna, zacisk w gnieździe, stanowisko badawcze, badania doświadczalne, symulacje komputerowe MES.

Streszczenie Celem pracy było doświadczalne i teoretyczne wyznaczenie wpływu najważniejszych parametrów wpływających na wartość momentu utwierdzenia cienkościennej panewki w gnieździe korbowodowym. W pierwszym etapie pracy zaprojektowano i wykonano stanowisko badawcze, na którym pomierzono rzeczywiste wartości momentów utwierdzenia dla różnych wariantów wykonania i montażu panewek w gnieździe, analizując również wpływ zaczepu. Następnie przeprowadzono badania teoretyczne z wykorzystaniem symulacji komputerowej MES.

ORIGIN AND AIM OF THE WORK

One of the failures occurring in modern engines is the rotation of a connecting rod bearing inside the housing bore. This generates significant repair costs due to the need to not only replace the bearing and regenerate the crankshaft, but also the connecting rod.

Theoretical knowledge concerning the choice and calculation of the required clamping force of the bearing in its housing and its impact on the torque which prevents the bearing's rotation is lacking and based mainly on the experience of manufacturers **[L. 1–3]**. The literature on this subject is remarkably inadequate. Although the authors have encountered a few studies on similar research issues, they concern only the damage of connecting rods, crankshafts **[L. 4–7]**, and bearings caused by factors other than bearing rotation (e.g., improper assembly) **[L. 8–11]**.

Some additional motivating factors behind this research included obtaining specific results for a tested bearing needed for an industrial application and an unambiguous clarification of the locking lip's function as a positioning feature, instead of a torque transferring element.

The purpose of the work was to experimentally and theoretically determine the impact of the main design parameters of a bearing shell and its assembly conditions on the value of the holding torque in

* ORCID: 0000-0003-2064-8739. Gdańsk University of Technology, Faculty of Mechanical Engineering, G. Narutowicza 11/12 Street, 80-233 Gdańsk-Wrzeszcz, Poland, e-mail: t.j.zochowski@gmail.com.
** ORCID: 0000-0003-0819-0980. Gdańsk University of Technology, Faculty of Mechanical Engineering, G. Narutowicza 11/12 Street, 80-233 Gdańsk-Wrzeszcz, Poland, e-mail: artur.olszewski@pg.edu.pl.

a housing bore. Both the friction between the bearing and the housing and the locking lip influence were taken into account.

DESCRIPTION OF THE RESEARCH ISSUE–A HALF SHELL INSIDE A CONNECTING ROD HOUSING BORE

Two bearing half-shells are assembled inside the connecting rod housing bore with each of them extending above the rod's parting face by a pre-determined value of a few hundredths of a millimetre (usually around 2 thousandths of the diameter). Two parts of the connecting rod are clamped with bolts (two or more) until their parting faces make contact. Because of their extensions, the shells deform, conforming to the housing bore. This deformation produces pressure on the bearing's outer surface, facilitating friction torque (which prevents the shell from rotating inside the bore).

A half-shell's extension beyond a connecting rod's parting face results from the difference between the lengths of its outer circumference and the half-circumference of the housing bore. This extension is known as *crushheight*, and it will be hereafter referred to as such. The relevant parameters are shown on **Fig. 1**.

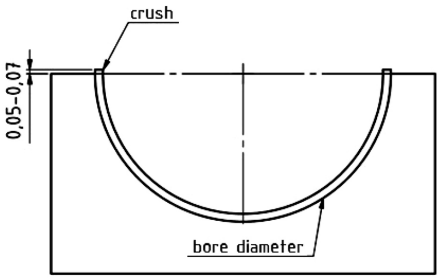

Fig. 1. Bearing crush of the researched connecting rod half-shell

Rys. 1. Wystawanie panwi ponad podział dla badanej półpanwi korbowodowej

Application of a proper clamping force should eliminate the possibility of the shell rotating inside the bore (consequently preventing damage to the bore) even under maximum engine torque (e.g., in the case of a seizure failure and adhesion of the bearing to the crankshaft journal).

Theoretically, two half-shells clamped inside the housing bore should produce a friction torque able to counteract the maximum engine torque generated on the crankshaft.

However, the ever-increasing loads present in modern combustion engines are not accompanied by a drastic increase of geometric dimensions of the engine parts (housing bore diameters, crankshaft diameters, bearing shell thickness etc.), which often precludes the above condition from being fulfilled. The main constraints on the maximum possible friction torque generated on the bearing shell are its thickness and material. Passing the yield point would result in a permanent deformation of the shell, preventing its subsequent assembly.

RESEARCH PLAN AND RESEARCH METHODOLOGY

The research plan has included test stand experiments and theoretical computer-assisted FEM simulations. The calculations were performed in the ANSYS Workbench 18.2 software.

A typical bearing shell was selected for testing, the parameters of which are shown in **Table 1**. Additionally, **Table 1** includes the relevant parameters of the bearing's source engine. **Fig. 2** depicts an axonometric view of the tested bearing half-shell with a semi-circular locking lip.

Table 1. Tested bearing parameters

Tabela 1. Parametry badanego łożyska

Shell outer diameter	74 mm
Shell width	29 mm
Shell thickness	2.2 mm
Locking lip diameter	5 mm
Locking lip protrusion	1.2 mm
Shell material	bimetal (low carbon steel + cast bronze layer)
Maximum engine torque	1100 Nm
Connecting rod housing material	steel

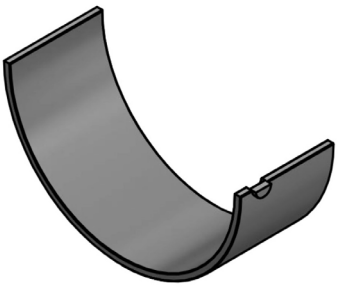

Fig. 2. Axonometric view of the tested bearing. Visible locking lip

Rys. 2. Poglądowy rzut aksonometryczny badanego łożyska. Widoczne zabezpieczenie kształtowe (zaczep)

Twenty-two half-shells were selected for testing (the maximum amount of samples was restricted by the project duration and cost), all originating from a single production series. Due to this, their circumferences differed by no more than 4 micrometres. The exact lengths are shown in **Table 2**. The circumferences of selected shells were deliberately modified in order to investigate the influence of various crush values, as indicated in the appropriate column.

Table 2. Tested bearings
Tabela 2. Badane łożyska

Shell no.	Total shell extension [mm]	Crush (half of total extension) [mm]	After modification [mm]	Notes
1	0.133	0.067	No modification	-
2	0.135	0.068	No modification	-
3	0.134	0.067	No modification	-
4	0.135	0.068	No modification	-
5	0.133	0.067	No modification	-
6	0.133	0.067	No modification	-
7	0.132	0.066	No modification	Shell after anti-corrosive treatment
8	0.133	0.067	No modification	Shell after anti-corrosive treatment
9	0.135	0.068	No modification	Shell after anti-corrosive treatment
10	0.135	0.068	No modification	Shell after anti-corrosive treatment
11	0.133	0.067	No modification	Oil on housing bore
12	0.135	0.068	No modification	Oil on housing bore
13	0.135	0.068	No modification	Oil on housing bore
14	0.134	0.067	No modification	Oil on housing bore
15	0.134	0.067	0	Parting face filed down
16	0.132	0.066	0	Parting face filed down
17	0.134	0.067	0	Parting face filed down
18	0.134	0.067	0	Parting face filed down
19	0.135	0.068	0.042	Partially lowered parting face
20	0.135	0.068	0.042	Partially lowered parting face
21	0.136	0.068	0.042	Partially lowered parting face
22	0.136	0.068	0.042	Partially lowered parting face

EXPERIMENTAL TESTS

The experimental tests were performed on a custom-designed, purpose-built test stand shown in **Fig. 3**. The stand consisted of a base **[L. 2]**, two supporting self-aligning spherical bearings **[L. 1]** enabling shaft rotation, a shell housing with a locking pin **[L. 4]**, and the main shaft transferring torque onto the tested shells **[L. 3]**. A special spanner **[L. 5]** was used to apply torque to the shaft, with calibrated weights hanged 2.09 m from the shaft axis in order to produce the desired moment of force.

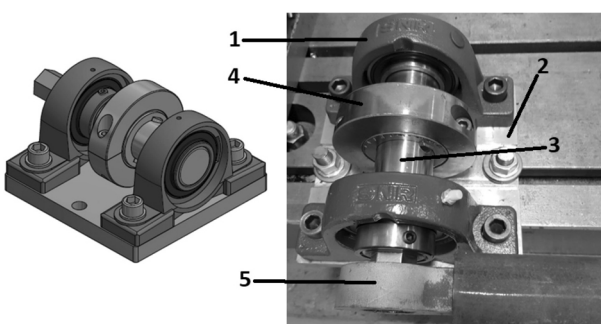

Fig. 3. Rendering of the test stand and the finished stand assembly
Rys. 3. Projekt 3D stanowiska oraz wykonany układ badawczy zamontowany na fundamencie

A problem that had appeared at the beginning of the research was the issue of transferring such high torque onto the thin-walled shells (shell thickness ~ 2.2 mm). After a series of unsuccessful tests using glue, a specially shaped connection was developed, allowing the transfer of the required torque without reducing the stiffness of the shell **(Fig. 4)**.

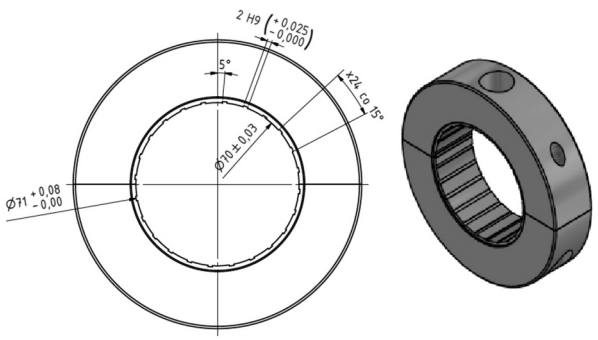

Fig. 4. Tested bearing modification allowing for torque transfer from the shaft onto the shell (front and axonometric views)
Rys. 4. Modyfikacja panwi badanych w celu przeniesienia momentu obrotowego z wału na panew (rzut aksonometryczny oraz od czoła panwi)

The torque was transferred through a special spline connection with 24 grooves placed 15 degrees apart, each 0.5 mm deep. The spline was angularly offset in order to ensure full contact between the half-shells on the parting face. Additionally, the inner diameters of the shells were reduced by 0.1 mm, which allowed partial compensation for the influence of the spline grooves. The design and its main dimensions are shown in **Fig. 4**.

The load acting on the spanner arm applying torque to the bearing was incrementally increased until the rotation of the shell inside the housing bore was achieved, after which, the torque range was noted (within +-4% margin of error), and the range of torque that can be applied in the stand is 90–950 Nm. The friction torque of the bearings in the housing is calculated from known mass that is acting on the arm of known length.

Because of the lengthiness and the high costs of manufacturing of the test bearings, it was necessary to reduce their number to the minimum required for the successful analysis and the comparison between the experiment outcomes and the simulation results.

Table 3 shows the results of the performed experiments. The test were divided into 5 main groups: a dry shell with full crush, a dry shell with a lowered crush, a shell with full crush and applied anti-corrosive treatment, and a shell with full crush and the bore covered with low-viscosity oil.

Most commonly, engine assembly manuals specify dry installation of bearing shells in order to achieve the desired fit. However, the surfaces are treated with an anti-corrosive agent, which (although wiped afterwards) remains on them in trace amounts. As demonstrated, even this treatment by itself leads to over 10% decrease of the friction torque.

The behaviour of a shell lubricated on the outer surface with low-viscosity oil (a common practice in car repair shops) has also been investigated. The lubricating effect is very pronounced, i.e. the substantial decrease of the friction coefficient leads to approximately 66% decrease of the friction torque when compared to a dry shell.

Observation of the rotation in the dry shell tests was slightly problematic; after exceeding a certain torque threshold, instead of rotating to the limit of the loading spanner, the shells would seize after only several degrees. As a solution to this, the shells were laser-marked and inspected after each load increase for any movement relative to a corresponding mark on the housing. As shown in **Table 3**, even for a dry shell, the friction torque amounts to approximately 75% of the maximum engine torque of 1100 Nm.

One of the main concerns of the research was the extent to which the locking lip is able to transfer torque. This was important in order to take this effect into account when calculating the friction torque, as well as to verify the common perception of the locking lip as an element preventing the rotation of the shell inside the housing bore. Simple calculations of the shorn cross-section area have indicated that the transferable torque is approximately 10 times lower than the maximum engine torque (about 130 Nm). In order to confirm these calculations, the shell was forcefully rotated in order to shear the lips (as shown on **Fig. 5**). The results have been included in **Table 3**. Both the theoretical and the experimental results show similar values.

Table 3. Experimental test results
Tabela 3. Wyniki badań doświadczalnych

	Friction torque	Notes
Shell without crash(locking lip only)		
Test 1 (bearing no. 15–16)	115–120 Nm	Shell rotates freely after shearing of the locking lip
Test 2 (bearing no. 17–18)	120–125 Nm	
0,067 mm crush(anti-corrosive treatment)		
Test 1 (bearing no. 7–8)	728.9–767.8 Nm	Shell rotates freely after exceeding the torque threshold
Test 2 (bearing no. 9–10)	678.2–743.9 Nm	
0.067 mm crush(oiled housing bore)		
Test 1 (bearing no. 11–12)	565.9–592.5 Nm	Shell rotates freely after exceeding the torque threshold
Test 2 (bearing no. 13–14)	458.5–520.2 Nm	
0.067 mm crush (dry)		
Test 1 (bearing no. 1–2)	754.8–760.2 Nm	Shell rotates several degrees and seizes. rotating again after slight application of torque
Test 2 (bearing no. 3–4)	794.2–801.2 Nm	
Test 3 (bearing no. 5–6)	810.2 – 830.6 Nm	
0.042 mm crush(dry)		
Test 1 (bearing no. 19–20)	562.5–604.5 Nm	Shell rotates several degrees and seizes, rotating again after slight application of torque
Test 2 (bearing no. 21–22)	>520 Nm (failed test)	

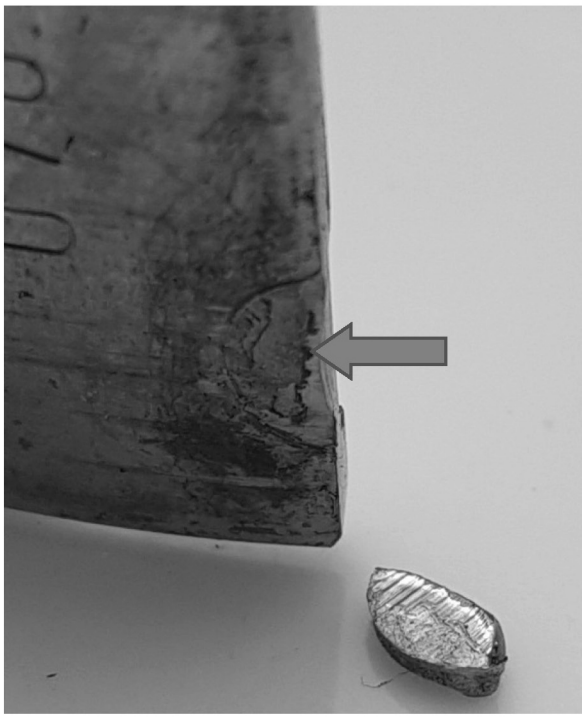

Fig. 5. Shorn locking lip
Rys. 5. Zerwany zaczep pozycjonujący panew w gnieździe

THEORETICAL INVESTIGATION

Computer-assisted simulations were performed independently from the experimental tests, which allowed the verification of the theoretical models, as well as their assessment as a tool for developing and designing new bearings.

In the FEM simulations, the housing was fixed on the outer surface (the thickness of the connecting rod is approximately 11 times higher than that of the thin-walled shell), and 4 different values of symmetric displacement (42, 48, 54, and 67 micrometres) were applied to both of the shell's contact areas. The values were selected in such a way as to allow the results to cover the entire tolerance range for the examined bearings (the 42 micrometre variant was slightly below the allowable tolerance). A frictional contact was defined between the housing bore and the shell (various values of the friction coefficient were tested to allow the theoretical calculations to be compared with the empirical tests).

The element mesh was generated with increased density around the contact areas. The contact edge was divided into 6 elements, and the element size parameter in the contact area was defined as 0.7 mm. A model consisting of 101900 nodes and 22248 elements was generated, ensuring detailed results as well as sensible processing time (under 15 minutes).

The nature of the investigated phenomenon has allowed us to exploit the symmetry of the model in order to expedite the calculations with the plane of symmetry dividing the housing's width. To ensure the validity of such an approach, several comparative calculations were performed with the full model. The results varied by no more than 0.5%.

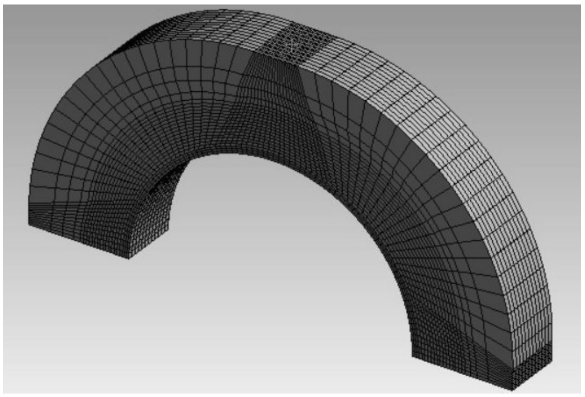

Fig. 6. Analyzed model mesh
Rys. 6. Widok siatki analizowanego modelu

The theoretical analysis has included both the cases investigated in the experimental tests, and additional variants were untested because of budget constraints. A preliminary analysis was performed in order to ensure the lack of interpenetration and the proper status of the contact elements. **Fig. 7** shows the penetration of the bodies to be limited to 0.2 micrometres, which is an acceptable value for calculations of this type.

The status of the contact elements was also determined to be correct. Interestingly, the size of the central surface **(Fig. 8)**, where the shell adheres closely to the housing bore (without movement), is virtually independent from both the coefficient of friction and the forced displacement of the shell contact area. The diameter of the contact area increases slightly towards the outside, which is caused by the utilized model symmetry (in a whole model the surface would be symmetrical) and by the shell's slight sideways shift during clamping, which is shown on **Fig. 9**. The shell's corner visibly deforms by a few micrometres in the axial direction (this behaviour is prevented on the other side of the shell because of the symmetry condition).

The stress and pressure distributions appeared similar independently of the assigned friction coefficient values. **Figures 10** and **11** show an example stress distribution in the shell and the pressure on the housing bore surface. The stresses were lowest in the middle area, increasing towards the contact edges. Notably, for maximum crush values, the stress near the contact edges approaches the yield point of the shell material (approx. 300 MPa), which indicates a deliberate design decision to maximize the holding torque without permanently deforming the shell during its assembly.

One of the additional phenomena investigated during the analysis was the reaction force on the shell contact surfaces resulting from their assembly. This allowed us to determine the characteristic of the force changing with respect to time, as well as to compare the

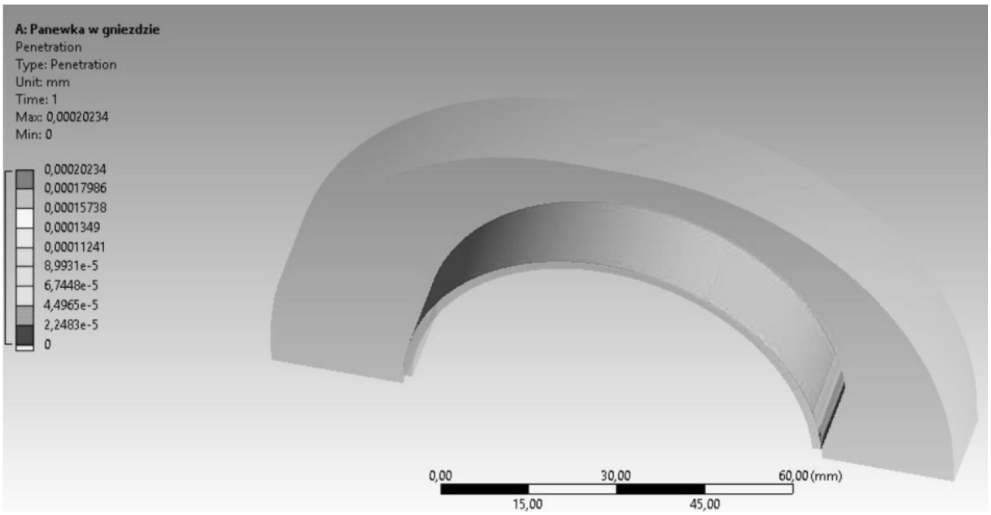

Fig. 7. Body penetration (shell and housing)
Rys. 7. Przenikanie się obu ciał (panwi i gniazda)

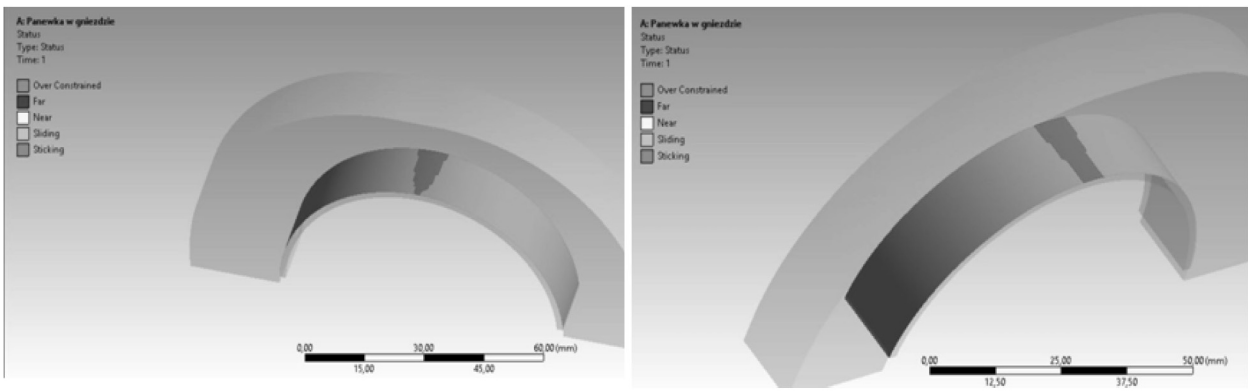

Fig. 8. On the right: contact status for the maximum values of crush height (67 micrometres) and friction coefficient (0.35); on the left: for the minimum values of crush (42 micrometres) and the friction coefficient (0.15)
Rys. 8. Po prawej stronie status elementów kontaktowych dla maksymalnego analizowanego wystawania (67 mikrometrów) oraz maksymalnego współczynnika tarcia (0,35), po lewej dla wystawania minimalnego (42 mikrometry) oraz minimalnego współczynnika tarcia (0,15)

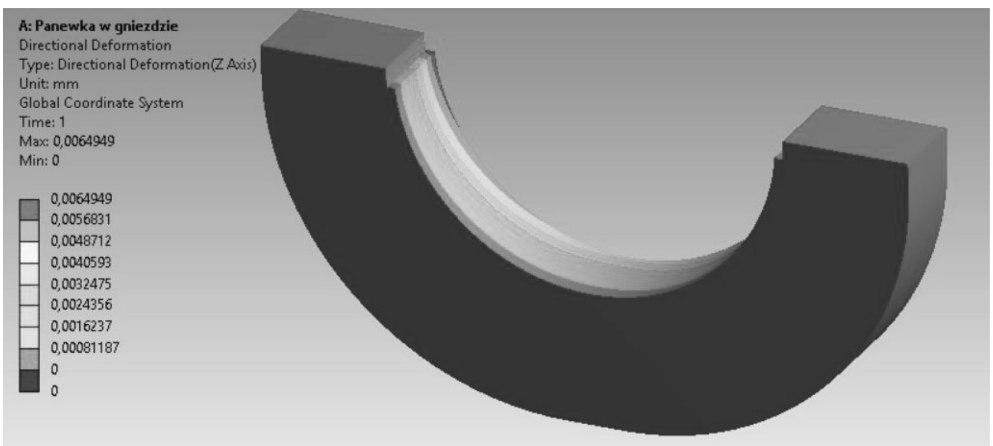

Fig. 9. Axial displacement (for crush height of 67 micrometres and friction coefficient of 0.3)
Rys. 9. Przesunięcie osiowe (dla wystawania 67 mikrometrów oraz współczynnika tarcia 0,3)

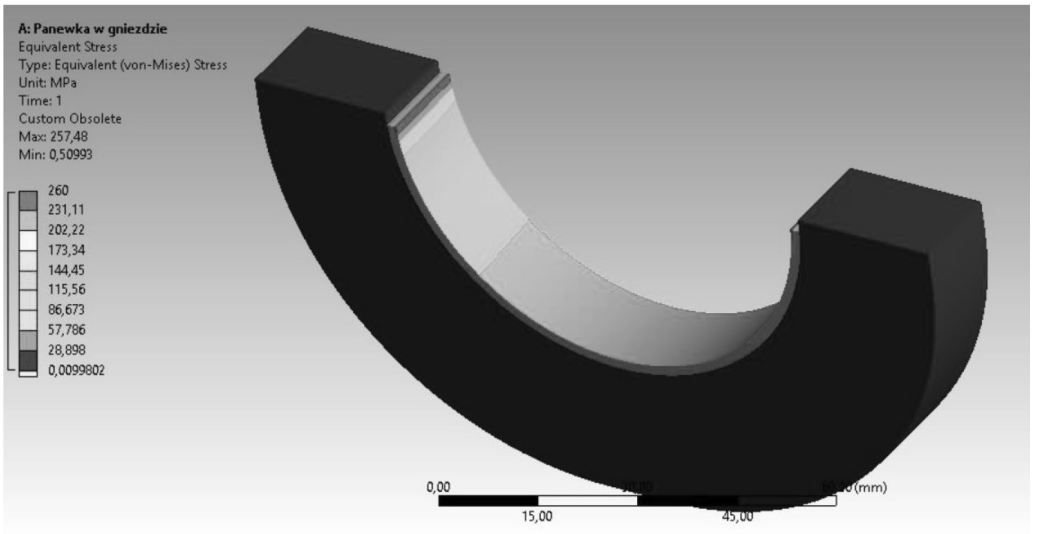

Fig. 10. Equivalent stress in the shell with crush height of 42 micrometres and friction coefficient of 0.25
Rys. 10. Naprężenia wywołane w panewce przy wystawaniu 42 mikrometry oraz współczynniku tarcia 0,25

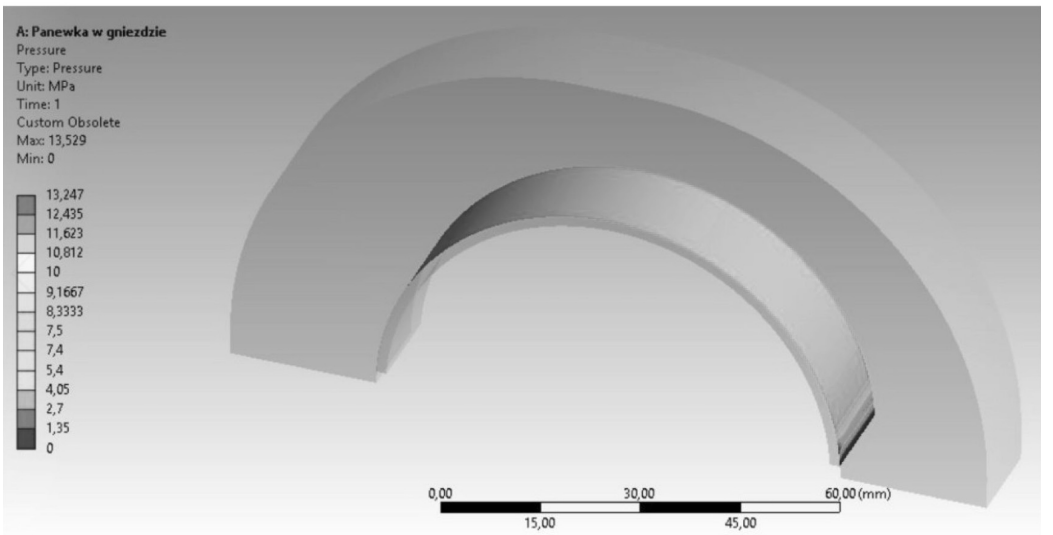

Fig. 11. Surface pressure on the housing bore with crush height of 42 micrometres and friction coefficient of 0.35
Rys. 11. Naciski na powierzchni gniazda przy wystawaniu 42 mikrometry oraz współczynniku tarcia 0,35

force needed to clamp the half-shells together with the force used in measurement bores during manufacturing inspection of this value.

Selected results of the analysis are shown on **Figs. 12, 13,** and **14**. The reaction force changes marginally depending on the friction coefficient with the difference between the extreme values for a single case amounting to approximately 14% with the maximum coefficient equalling 233% of the minimum one.

The behaviour of the pressure distribution characteristic is similar **(Fig. 13)** (difference under 5%). Slight deviations of the determined mean pressure values result from the averaging error.

Demonstrably, the value of the coefficient of friction has a limited impact on the reaction forces and the pressure acting on the housing bore. However, it has tremendous influence on the friction torque (which is simply proportional to its value).

SUMMARY AND CONCLUSIONS

- The conducted research has allowed us to experimentally and theoretically evaluate the influence of a bearing shell's fundamental design parameters and assembly conditions on the value of its holding torque. Both the friction force on the contact surface between the shell and the housing bore and the influence of the locking lip were taken into account.

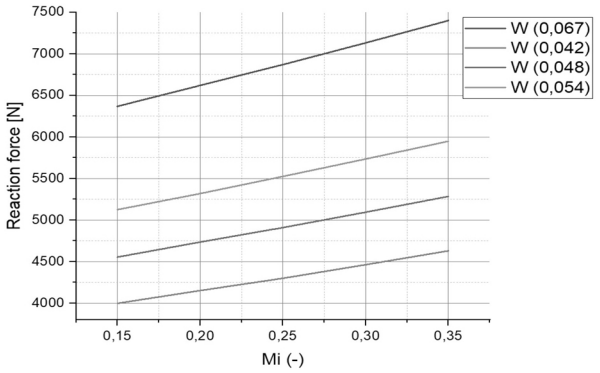

Fig. 12. Reaction force (single contact) as a function of the friction coefficient for various bearing crush height values

Rys. 12. Siły reakcji (pojedynczy styk) w zależności od wartości współczynnika tarcia pomiędzy panewką i gniazdem dla różnych wartości wystawania panewki

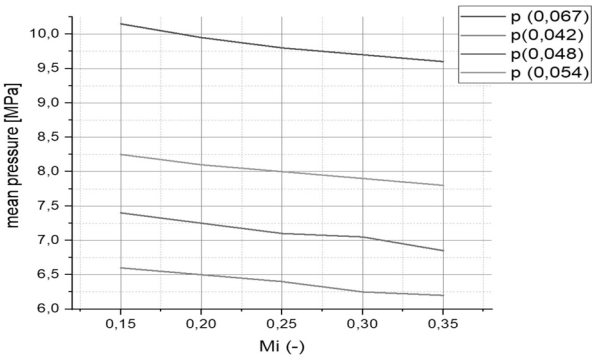

Fig. 13. Mean pressure on housing bore surface as a function of friction coefficient for various bearing crush height values

Rys. 13. Średnie naciski na powierzchni gniazda w zależności od wartości współczynnika tarcia pomiędzy panewką i gniazdem dla różnych wartości wystawania panewki

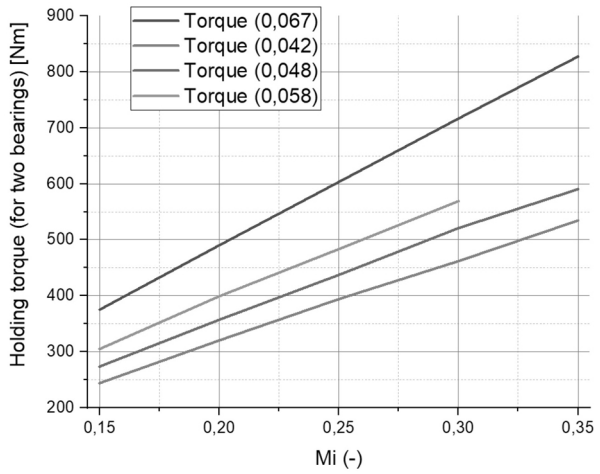

Fig. 14. Friction torque as a function of friction coefficient for various bearing crush height values

Rys. 14. Wartości momentów oporowych dla różnych wartości współczynnika tarcia oraz różnych wartości wystawania ponad podział

- The experimental tests and the theoretical analysis allowed us to establish a correlation between the calculations and the experiments. The friction torque of a shell with decreased crush amounts to 73% of the torque for a bearing with the highest crush. Although the calculations result in a 65% value instead, the 8 percentage point difference seems negligible when considering all of the various factors contributing to measurement uncertainty.
- The value of the coefficient of friction has limited impact on the reaction forces on the contact faces and the pressure acting on the housing bore. However, it has tremendous influence on the friction torque (which is simply proportional to its value). The characteristics resulting from the performed computer simulations display a nearly linear behaviour and can be extrapolated for values beyond the original data range.
- The computer simulation results follow the experimental findings when the coefficient of friction equals approx. 0.33 to 0.34, which is a reasonable value for steel-on-steel contact. For the shell oiled during assembly, the coefficient equals 0.22, which is also possible considering the miniscule amount of the lubricant and the relatively high pressures.
- The results indicate that, because of the high torque values achieved in modern engines, it is impossible to prevent the bearing shell from rotating inside the bore in the case of a seizure failure. The only means of protecting the bearing from the above danger is the employment of other design solutions (improved materials, thicker shell cross-sections, wider shells) which are currently not feasible because of their detrimental influence on other issues related to manufacturing, costs, and engine operation.
- The experimental results provide a relatively large range of values despite the rigorous dimensional requirements for the tested bearings. This is caused by uncontrollable factors such as the micro-damage of the housing bores after previous tests, surface roughness changes resulting from polishing of minor scratches, the imprecision of assembly, etc.
- The authors would like to emphasize that the research has not been conducted on a scale wide enough to merit the generalization of its conclusions. The research is a preliminary step towards further planned investigations. A larger-scale research is planned in the future, utilizing an improved measurement method. A higher number of tests would be advised, which was unfortunately impossible at this time due to high cost and labour intensity of the sample bearings. In order to mitigate this, the simplification of future samples is intended.

ACKNOWLEDGEMENTS

The authors would like to express their gratitude to Federal-Mogul Bimet S.A and the Faculty of Mechanical Engineering of Gdańsk University of Technology for financing the conducted research.

REFERENCES

1. Clevite (Mahle) Catalog No. EB-10-07 2007/2008.
2. KatalogMotorserviceRheinmetall Automotive: Uszkodzenia łożysk ślizgowych, MS Motorservice International GmbH 2017.
3. Clevite – Mahle Aftermarket: Engine Bearing: Failure Analysis and Correction, Technical Information.
4. Mateusa J., Anesa V., Galvãoa I., Reis L.: Failure mode analysis of a 1.9 turbo diesel engine crankshaft Engineering Failure Analysis 101 (2019), pp. 394–406.
5. Ligier J-L and Dutfoy L.: Fatigue prediction for engine bearing, Prévision de la tenuemécanique d'un coussinet 10th EDF/Pprime Workshop, Poitiers 2011.
6. Gomes J., Gaivota N., Martins R.F., Silva P.P.: Failure analysis of crankshafts used in maritime V12 diesel engines; Engineering Failure Analysis 92 (2018), pp. 466–479.
7. Fontea M., Freitasb M., Reis L.: Failure analysis of a damaged diesel motor crankshaft Reisb Engineering Failure Analysis 102 (2019), pp. 1–6.
8. Bouyer J., Fillon M.: An experimental analysis of misalignment effects on hydrodynamic plain journal bearing performances. ASME J. Tribol. 2002;124:313–9.
9. Sun J., Gui C.L., Li Z.Y.: Influence of journal misalignment caused by shaft deformation under rotational load on performance of journal bearing. Proc. Inst. Mech. Eng, Part J.: J. Eng. Tribol. 2005;219, pp. 275–83.
10. Jang J.Y., Khonsari M.M.: On the relationship between journal misalignment and web deflection in crankshafts. J Eng Gas Turbines Power 2016;138(122501), pp. 1–10.
11. Martin F.A. Developments in engine bearing design. TribolInt 1983;16, pp. 147–64.